Regional Inertia Estimation Using Actual Event Measurements: Florida Case

Saurav Dulal[1], Mohammed M. Olama[2], Ali R. Ekti[2], Nils M. Stenvig[2], and Yilu Liu[1,2]
[1] Department of Electrical Engineering and Computer Science
The University of Tennessee, Knoxville, TN, USA
[2] Oak Ridge National Laboratory, Oak Ridge, TN, USA
(emails: sdulal@vols.utk.edu, olamahussemm@ornl.gov, ektia@ornl.gov, stenvignm@ornl.gov, liu@utk.edu)

***Abstract*—As inverter-based resources' integration in power grids increases, their uneven distribution across the electrical network leads to the formation of local regions that are weakly coupled to the larger interconnection. This signifies the necessity of regional frequency dynamics investigation and analyzing various inertia metrics. This paper presents a practical methodology for estimating regional rate-of-change of frequency (RoCoF) using actual event recordings, which is then used to evaluate regional inertia. Florida (FL) is selected as the region of interest due to its distinct regional frequency dynamics and the rising levels of solar generation. We identify and analyze confirmed events from 2017 to 2024 that occurred in FL. The results indicate that FL contributes about 14% to the total inertia of the US Eastern Interconnection, which approximately matches its share of generation capacity. Results also highlight seasonal fluctuations in energy generation, which play a significant role in influencing inertia and thus the RoCoF levels. This emphasizes the importance of estimating regional inertia to enhance grid operations for a future that focuses on distributed generation.**

***Index Terms*—Florida, inverter-based resources (IBRs), rate-of-change of frequency (RoCoF), regional inertia**

I. Introduction

As inverter-based resources (IBRs) become more prevalent, they contribute to a noticeable decline in the system's overall inertia. This decline in inertia may lead to a lower frequency nadir and an elevated rate-of-change of frequency (RoCoF). Such changes can inadvertently activate under-frequency protective devices [1]. IBRs are spread unevenly, which causes some areas to become weakly connected to others. This results in a reduction of dynamic coupling between the region and the wider interconnection. Consequently, the inertial support that each region receives from the entire system is restricted [2].

The inertia estimation results in [3]–[6] suggest that the interconnection-level inertia in the United States (US) is not declining in the past decade as expected, and it may be enough to limit the interconnection RoCoF to an acceptable level during any contingency. However, the local and regional RoCoF might cross the equipment's designed thresholds. This may result in cascaded loss of generators, starting from the low-inertia regions and spreading to the whole interconnection. Therefore, there is an urgent need to estimate the regional inertia for situational awareness and to plan some mitigation measures.

Existing methods for inertia estimation can be broadly categorized as model-based and measurement-based methods. The most common model-based method includes an inertia summation approach that adds the inertia of all online generators [5]. This method is limited because it excludes the inertia from both IBRs and the load. Instead, the measurement-based method uses data collected by phasor measurement units (PMUs). These data can come from regular grid activity, probing signals, or actual disturbance events. The ambient data approach relies on normal load changes in the grid; however, this approach requires filtering out the noise from the data, and this process leads to inaccurate results with added complexity. The probing approach, such as [7], is invasive and requires additional investment and configuration for devices to probe signals into the grid.

The event-driven approach estimates system inertia by analyzing system frequencies and power fluctuations that occur during major grid disturbances. Although the events can be limited in number, they help in yielding effective inertia values that include contributions from synchronous generators (SGs), IBRs and load, thus, serving to obtain a more accurate inertia estimate. As compared to the ambient and probing approaches, the event-driven approach reveals how the system truly responds under stressful conditions. Furthermore, the use of real event data in inertia evaluation helps in capturing the subtle real power system behavior that is difficult to capture using modeling-based methods. Other methods include machine learning applications such as in [8], where features from PMU measurements are extracted to estimate the inertia. However, this is a black box method that needs a huge amount of data to train the model.

This paper introduces an event-driven approach for evaluating the regional inertia by estimating the RoCoF using actual event data. The approach integrates frequency responses from all generation sources connected to the region's power system. First, an electrical region is identified within the Eastern Interconnection (EI). Then, a RoCoF estimation technique is

applied to calculate the region's RoCoF. The obtained result is used to calculate the inertia of the region. Florida (FL) is selected as an interesting use case in this study for estimating its regional grid inertia due to its distinct regional frequency dynamics and the rising levels of renewable generation.

The remaining sections of the paper are organized as follows: Section II outlines the approach for identifying a region and introduces key concepts related to regional inertia; Section III details the source of frequency measurements used; Section IV describes the methodology for estimating regional inertia; and Section V provides the estimation results and compares them with interconnection-wide values. Finally, the paper highlights major findings and suggests potential directions for future research in section VI.

II. Regional Inertia Concept

A. Region Identification

When a generation trip event occurs in an area that is weakly coupled to the rest of the interconnection, the region might experience substantial swings of frequency around the central frequency of the system [9]. In areas close to the event location, where coupling to the broader interconnection is weak, frequency sensors detect a sharper and earlier frequency drop. In contrast, frequencies in other areas drop more gradually. This behavior can help locate a region by examining how frequency responses vary with connection strength and distance from where the event occurred.

The real case, depicted in Fig. 1, further exemplifies such dynamics. The generators in FL show a steep frequency decline before other regions begin to experience any change. This indicates that FL may be somewhat decoupled from the rest of the system. This weaker coupling is evidenced by the large frequency swings around the central frequency, as indicated by measurements in FL, with the interconnection frequency represented by the black curve. The other areas such as GA, SC, NC, AL, TN, NY, VA, etc., however, seem more tightly integrated with the interconnection. This is because the frequencies in these areas exhibit a more gradual and delayed frequency decline. This lag happens because inertial forces from across the interconnection take time to propagate over the wide area to the event's origin point. These insights depict how analyzing frequency dynamics can help identify weakly coupled regions like FL.

B. Inertial Response

SGs can inherently provide kinetic energy from their rotating mass whenever there is a mismatch between the load and generation due to a system event. The ability to provide kinetic energy and oppose the change in frequency is referred to as inertial response. The equation that governs these dynamics is the swing equation, which can be simplified as [10], [11]:

$$\frac{df_i}{dt} = \frac{P_{mi} - P_{ei}}{2H_i S_i} f_s \tag{1}$$

where the system has n number of connected generators, f_i is the frequency of i^{th} individual generator, f_s is the nominal

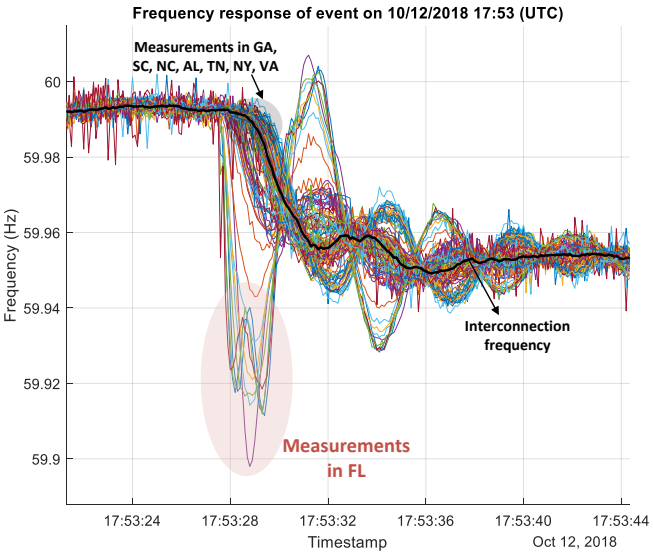

Fig. 1. A generation outage illustrating the frequency changes across the whole eastern interconnection.

system frequency, P_{mi} and P_{ei} is the mechanical and electrical power respectively, H_i represents inertia constant, S_i indicates rated capacity of the generator, and $i = 1, ..., n$.

For a group of generators within a defined electrical area, the swing equation describes this behavior as:

$$\frac{df_{reg}}{dt} = \frac{P_m - P_e}{2H_{reg}S_{reg}} f_s = \frac{\Delta P}{2H_{reg}S_{reg}} f_s \tag{2}$$

where the power imbalance between load and generation is given by ΔP, the central frequency of the region is represented by f_{reg}, H_{reg} is the inertia of the region, and S_{reg} represents the system capacity of the region. f_{reg} is calculated as the weighted average of local frequencies from multiple areas as [12]:

$$f_{reg} = \frac{\sum_j^m w_j f_j}{\sum_j^m w_j} \tag{3}$$

The weight w_j indicates how much inertia each area contributes within a region. In real-world use, it's necessary to rely on generator-specific information—such as rated power or inertia constants—to determine these weights. One common method is to estimate weights based on the product of a generator's rated output and its inertia constant. However, accurately tracking generator dispatch data during actual events is often difficult. To simplify the process, it's sometimes assumed that all areas have the same weight. While convenient, this assumption can lead to a slight over- or underestimation of the system's actual inertia.

III. Frequency Measurement

This work utilizes frequency data sourced from FNET/GridEye, a network consisting of over 300 Frequency Disturbance Recorders (FDRs) distributed throughout the US. These devices capture high-resolution frequency, voltage, and

phase angle information from various locations. The study focuses on past event data recorded by the FDRs, which is stored on servers hosted at University of Tennessee, Knoxville and Oak Ridge National Laboratory [13].

IV. Practical Methodology for Regional Inertia Extraction

Once the coherent group of generators is observed through the visual inspection of frequency clusters, as in Fig. 1, we can identify a region. Following the region identification process, the steps shown in the proposed flow chart in Fig. 2 are carried out for the regional inertia estimation.

A. Regional Frequency

The frequency data collected by the FDRs in a specific region are used to calculate the central or regional frequency of that region. This value is determined using the formula provided in expression (3). The frequency data, denoted as f_i, is given by the frequency measured by the different FDRs. The frequency estimate obtained using such an averaging method helps in filtering the measurement noise and impact of outlier readings. Fig. 3 shows the regional frequency dynamics captured during a generation trip event. The black curve represents the regional frequency and the other curves illustrated by multi-colors are the frequency curves from different parts of the region.

B. Event Point Detection

In order to precisely compute the RoCoF, we need to first detect the event start point (time). In Fig. 3, the event point is represented by Point "A". The event point in the curve is the point after which there is a sharp drop in frequency. Therefore, to determine such a turning point when an event takes place, we compute the difference between the following two successive RoCoF and choose the maximum as:

$$RoCoF_{Diff} = max\,|RoCoF(t)_{pre} - RoCoF(t)_{post}| \quad (4)$$

where $RoCoF(t)_{pre}$ is the RoCoF calculated using the frequency points represented by yellow and red colors in Fig. 3. These points are separated by a time window of Δt. Similarly, $RoCoF(t)_{post}$ is determined using the frequency points represented by red and blue colors in the figure. The frequency point which has the maximum difference between pre-RoCoF and post-RoCoF is chosen as point "A". This technique gives us the most significant change in RoCoF. And, this represents the event start point for a given frequency curve during an event.

We have computed the value of $RoCoF_{Diff}$ for each point within a specific time period. This period starts from 8-10 seconds before the event. This is conducted to avoid capturing sudden unwanted frequency spikes from sensors during the event detection process.

C. RoCoF Estimation

RoCoF estimation methods can either be non-window-based or window-based methods. Non-window-based methods process data continuously and are more vulnerable to the transient noise. In contrast, window-based methods are known for their greater accuracy in estimating RoCoF due to their ability to filter out noise by segmenting data into multiple intervals [14]. However, window-based methods can have different window sizes based on the inertia of the target power system network. The proposed approach is a hybrid method, which leverages the strengths of both methods. Specifically, the frequency estimate is carried out using the average of the frequency measurements from all FDRs, which effectively mitigates the impact of minor noises. The noise reduction is the main strength of window-based methods, while the continuous calculation of RoCoF utilizing the moving 0.1 second time window ensures high temporal resolution, which is a key feature of non-window-based methods. Uniquely, the generation trip in a large power system generally does not induce the frequency spikes, which further ensures stable RoCoF estimation [14]. In this proposed methodology, RoCoF is calculated using the moving time window within 0.5 second, according to the NERC (North American Electric Reliability Corporation) standard [15].

A finer time window of 0.1 sec (which is the smallest interval) is used to calculate the RoCoF between the two points following the event onset time, as determined in Section IV. B. These points are represented by green colors in Fig. 3. The point having the maximum RoCoF within the 0.5 sec after point "A" is selected for calculating event regional RoCoF. This value is then used for further calculation of regional inertia. By combining noise reduction (via FDR averaging) with high-resolution RoCoF tracking during the most dynamic post-event phase, the hybrid method balances accuracy and responsiveness. As a result, it is a robust solution for analyzing regional power system dynamics during critical events.

D. Inertia Estimation using Real Events

To estimate regional inertia using real events, in addition to the previously calculated RoCoF, only the power imbalance data is needed. This power mismatch information is sourced from a verified NERC list of events, that includes MW sizes and locations. Only events within the targeted region are considered to ensure relevance. By observing how frequency changes during such events, the inertia of that specific region is estimated. Equation (5) shows the rearranged formula used, and the resulting inertia is expressed in MVA·s, a common unit for energy-related inertia.

$$H_{reg}S_{reg} = \frac{\Delta P}{2\frac{df_{reg}}{dt}} f_s \quad (5)$$

V. Inertia Results and Analysis: Florida Case

In 2023, more than 8.5% of the country's utility-scale solar energy was generated in FL [16]. This ranked the state third in

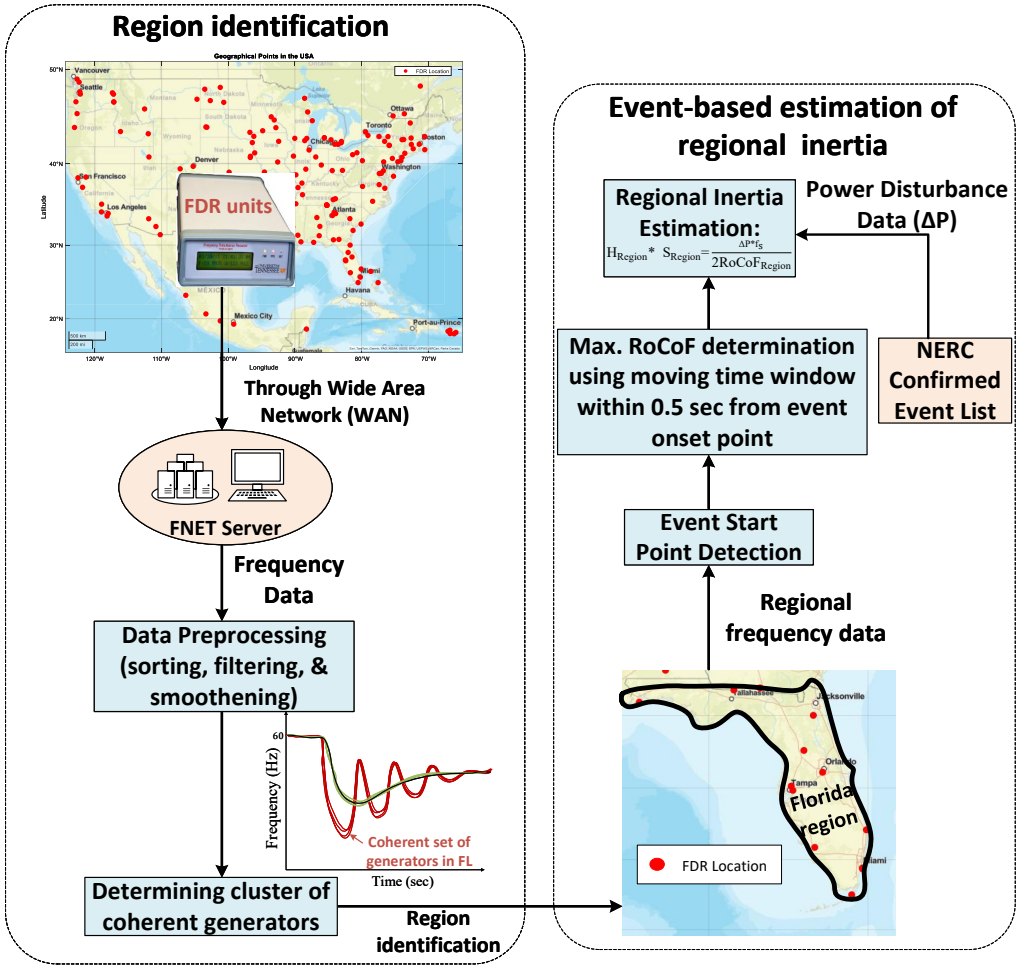

Fig. 2. The proposed framework for regional inertia estimation.

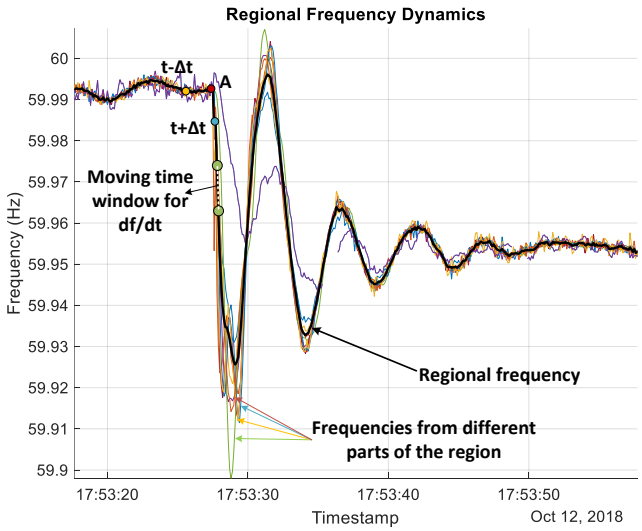

Fig. 3. Regional frequency dynamics illustrating the event start point and moving time window RoCoF calculation.

the nation for solar energy production [16], [17]. As FL continues to reduce coal-fired generation and invest in renewable like solar (planning to double its solar capacity between 2023-2026 [16]), the region's inertia has become a growing concern. As of the latest energy portfolio assessment [18], Florida's total installed solar capacity has reached approximately 14%, as depicted in the generation breakdown pie chart illustrated in Fig. 4. The state's location at the southeastern tip of the US creates a geographical barrier, with limited high-capacity transmission lines connecting it to neighboring states. This restriction hinders FL's integration into the larger electrical grid and increases its vulnerability to local disturbances. FL imported less than 3% of the needed electricity in 2022 [17], demonstrating an increasing reliance on in-state generation. This underscores the necessity for regional inertia estimation, which helps grid operators assess the grid's ability to respond to disturbances. Additionally, the state's frequent exposure to hurricanes and tropical storms further highlights the importance of accurately estimating regional inertia.

From 2017 to 2024, thirteen verified events took place in FL. Table I provides detailed inertia results from these events using power mismatch data from NERC. It lists key parameters such as local and regional RoCoF, local and regional inertia, and the time it takes for inertia support to arrive. The local RoCoF is derived from the FDR closest to where the event began. This initial frequency drop, before recovery, captures the dynamics

TABLE I
COMPREHENSIVE INERTIA EVENT ANALYSIS FOR FLORIDA REGION

Event Number	1	2	3	4	5	6	7	8	9	10	11	12	13
Event Date (UTC)	9/8/2017 17:31	9/10/2017 22:55	1/25/2018 02:47	5/22/2018 17:43	10/12/2018 17:53	10/29/2018 17:16	3/18/2019 23:58	3/30/2019 00:35	4/25/2019 13:18	7/5/2019 20:00	10/6/2022 03:16	5/12/2023 23:19	06/10/2024 14:00
Power Mismatch (MW)	757	770	370	757	994	971	540	511	1000	850	505	570	650
Interconnection RoCoF (mHz/s)	6.7	10.8	5.9	6.3	13.4	13.9	7.2	5.9	14.5	6.0	6.7	8.2	4.6
FL RoCoF (mHz/s)	26.7	11.9	30.3	44.4	12.4	103.1	56.1	58.4	135.0	31.3	45.8	54.5	19.8
Local RoCoF (mHz/s)	57	190	97	104	397	268	84	184	382	134	94	204	86
H_{intercon} (MVA·s)	$3.42 * 10^6$	$2.14 * 10^6$	$1.90 * 10^6$	$3.60 * 10^6$	$2.23 * 10^6$	$2.10 * 10^6$	$2.25 * 10^6$	$2.61 * 10^6$	$2.08 * 10^6$	$4.27 * 10^6$	$2.53 * 10^6$	$2.09 * 10^6$	$4.22 * 10^6$
H_{FL} (MVA·s)	$8.50 * 10^5$	$1.95 * 10^5$	$3.67 * 10^5$	$5.11 * 10^5$	$2.40 * 10^5$	$2.83 * 10^5$	$2.89 * 10^5$	$2.63 * 10^5$	$2.22 * 10^5$	$8.16 * 10^5$	$3.31 * 10^5$	$3.14 * 10^5$	$9.85 * 10^5$
H_{local} (MVA·s)	$3.98 * 10^5$	$1.22 * 10^5$	$1.14 * 10^5$	$2.18 * 10^5$	$7.51 * 10^4$	$1.09 * 10^5$	$1.93 * 10^5$	$8.33 * 10^4$	$7.85 * 10^4$	$1.90 * 10^5$	$1.61 * 10^5$	$8.38 * 10^4$	$2.26 * 10^5$
Inertial Support Arrival Time (s)	0.9	1.5	0.8	1.1	1.1	1.1	1.0	0.7	0.9	1.4	0.7	0.9	1
$H_{\text{FL}}/H_{\text{intercon}}$ (%)	24.9	9.11	19.3	14.2	10.8	13.5	12.8	10.1	10.7	19.1	14.7	15.0	23.3

specific to the area. The regional RoCoF reflects system-wide behavior across FL and is computed using all FDR data. The first episode of the frequency decline before the recovery can be analyzed by capturing the frequency dynamics from the closest FDR. This allows for the determination of local RoCoF and thus, local inertia. The regional RoCoF reflects the RoCoF of the entire FL region. It is obtained from the regional frequency that utilizes data from all the FDRs deployed in FL. For the regional RoCoF, a moving RoCoF approach is employed as described in Section IV.C.

The inertia support arrival time is the time difference between when the local frequency drops and when the interconnection frequency does. This indicates how quickly support reaches the region. For FL, this time is about one second, meaning inertial support from the EI arrives roughly one second after an event. The interconnection frequency begins to drop about one second after the disturbance occurs in the FL region, highlighting the response time for inter-area inertial support. The interconnection inertia is estimated using the RoCoF derived from the interconnection frequency behavior. The method follows the approach described in [4] to compute the interconnection inertia. As shown in the last row in Table I, FL contributes approximately 14% to the total inertia of the EI; this is also illustrated in Fig. 5.

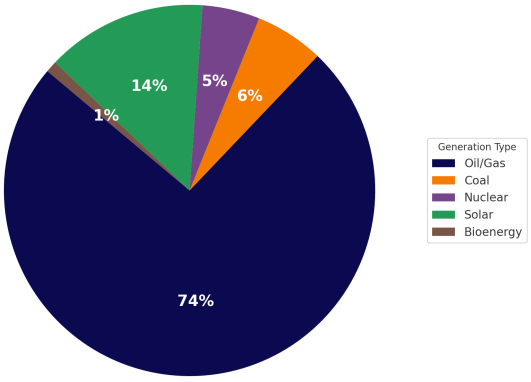

Fig. 4. Percentage share of installed capacity by generation type.

The total generation capacity of the whole EI is around

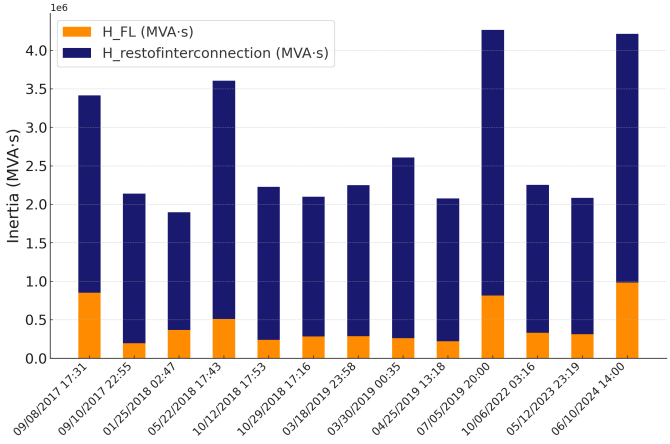

Fig. 5. Estimated inertia of Florida and Eastern Interconnection using the event-based approach. The stacked bars show Florida's relative contribution across multiple disturbance events.

700 GW [18]. While for FL, it is around 70 GW [17], which suggests that FL contributes about 10% to the total generation capacity of EI. The close match between generation capacity share and inertia contribution indicates that the event-based estimation method provides reasonably accurate results. Minor discrepancies may occur due to variations in fuel types across different regions or specific dispatch decisions during the event. Additionally, the analysis shows that inertia values tend to be highest during the summer months. This is because summer months are known to have the highest generation commitment among all.

For example, Event 10 (July 5, 2019) occurred in summer with an 850 MW mismatch, yielding a relatively low FL RoCoF of 31.3 mHz/s. This lower RoCoF value can be attributed to the higher regional inertia from a greater number of online conventional generation units. In contrast, Event 8 (March 30, 2019) had a smaller mismatch (511 MW) in spring (during low demand), when system inertia tends to be lower due to reduced generation commitment. Despite the smaller mismatch, the regional RoCoF nearly doubled to 58.4 mHz/s, reflecting the impact of lower inertia. Notably, Event 13 (June 10, 2024) had the highest regional inertia. This may be explained by the

fact that the event occurred on a summer afternoon, a period often associated with elevated system demand and higher synchronous generation commitment. Even during periods of high solar output, these circumstances highlight the role of regional inertia in reducing frequency excursions.

VI. Conclusion

This study introduces a practical, event-driven approach for estimating RoCoF and evaluating regional inertia. The process begins by identifying coherent generator groups during disturbance events to define the electrical region of interest—FL in this study. Regional frequency is then computed using measurements from FDRs located within the selected area. A specialized event detection algorithm is used to pinpoint the onset of the event based on frequency trends. To ensure precise RoCoF estimation, a hybrid method is employed that merges the noise-filtering strengths of window-based techniques with the high temporal resolution of non-window-based ones.

Inertia-related metrics were calculated for all verified events and are summarized in Table I. This study highlights key insights, particularly regarding the interaction between solar generation, regional inertia, and frequency dynamics. The analysis suggests that increased solar penetration may result in higher local RoCoF values during disturbances, particularly during low-demand periods when fewer synchronous generators are online. These outcomes highlight the importance of deploying frequency support mechanisms, such as demand response and energy storage, especially during seasonal variations in generation patterns across Florida.

While this methodology was demonstrated in a region with noticeable frequency characteristics, it is adaptable to other power systems with proper identification of coherent zones and corresponding frequency data. Future work will focus on enhancing the region identification process and refining the estimation approach, following methods such as those outlined in [19], as well as extending the applicability of this framework to other regions.

Acknowledgment

This material is based upon work supported by the US Department of Energy, Office of Electricity (OE) under contract DE-AC05-00OR22725.

References

[1] L. Zhu, E. Farantatos, D. Ramasubramanian, P. Mitra, V. Singhvi, and M. Elnasry, "Ambient PMU measurements based online regional inertia estimation and monitoring," in *2024 International Conference on Smart Grid Synchronized Measurements and Analytics (SGSMA)*, 2024, pp. 1–5.

[2] G. Misyris, B. Graham, P. Mitra, D. Ramasubramanian, and V. Singhvi, "Methodology for identifying regional inertia issues in future power grids," in *2023 IEEE Power & Energy Society General Meeting (PESGM)*, 2023, pp. 1–5.

[3] C. Zhang, "Measurement-based monitoring and control in power systems with high renewable penetrations," Ph.D. dissertation, University of Tennessee Doctoral Dissertation, 2023.

[4] S. Dulal, C. Zhang, M. Baldwin, Q. Liu, M. M. Olama, N. M. Stenvig, N. Bhusal, A. Yadav, and Y. Liu, "Measurement-based approach for inertia-trend analysis of the US Western Interconnection," in *2024 IEEE Kansas Power and Energy Conference (KPEC)*, 2024, pp. 1–6.

[5] P. Du, *Renewable Energy Integration for Bulk Power Systems: ERCOT and the Texas Interconnection*. Springer Nature, 2023.

[6] S. Dulal, C. Zhang, M. Olama, Q. Liu, N. Bhusal, A. P. Yadav, M. Baldwin, N. Stenvig, and Y. Liu, "Inertia estimation and trend analysis of the united states power grid interconnections," *IEEE Access*, 2024.

[7] Z. Jiang, H. Yin, H. Li, Y. Liu, J. Tan, A. Hoke, B. Rockwell, and C. Kruse, "Probing-based inertia estimation method using hybrid power plants," in *2023 IEEE Power & Energy Society General Meeting (PESGM)*, 2023, pp. 1–5.

[8] Y. Cui, S. You, and Y. Liu, "Ambient synchrophasor measurement based system inertia estimation," in *2020 IEEE Power & Energy Society General Meeting (PESGM)*, 2020, pp. 1–5.

[9] E. Farantatos, P. Dattaray, and M. Patel, "PMU based inertia estimation and monitoring," Apr. 2021. [Online]. Available: https://naspi.org/sites/default/files/2021-04/D1S1_01_farantatos_epri_naspi_20210413.pdf

[10] P. Wall, F. Gonzalez-Longatt, and V. Terzija, "Estimation of generator inertia available during a disturbance," in *2012 IEEE Power and Energy Society General Meeting (PESGM)*, 2012, pp. 1–8.

[11] P. Kundur, *Power System Stability and Control*. CRC Press New York, 2007.

[12] Y. Zhao and Y. Liu, "Real-time inertia estimation using probing method and PMU measurement," 2024.

[13] Y. Zhang, P. Markham, T. Xia, L. Chen, Y. Ye, Z. Wu, Z. Yuan, L. Wang, J. Bank, J. Burgett *et al.*, "Wide-area frequency monitoring network (FNET) architecture and applications," *IEEE Transactions on Smart Grid*, vol. 1, no. 2, pp. 159–167, 2010.

[14] H. Yin, Y. Wu, W. Qiu, C. Zeng, S. You, J. Tan, A. Hoke, C. J. Kruse, B. W. Rockwell, K. A. Kawamura, and Y. Liu, "Precise ROCOF estimation algorithm for low inertia power grids," *Electric Power Systems Research*, vol. 209, p. 107968, 2022. [Online]. Available: https://www.sciencedirect.com/science/article/pii/S0378779622001985

[15] NERC, "Frequency response standard background document," Jan. 2012. [Online]. Available: https://www.nerc.com/pa/stand/frequency%20response%20project%20200712%20related%20files%20dl/bal-003-1-background_document-redline_20120210.pdf

[16] SEIA, "State overview- Florida," Aug. 2024. [Online]. Available: https://seia.org/state-solar-policy/florida-solar/

[17] EIA, "Florida state profile and energy estimates," Feb. 2024. [Online]. Available: https://www.eia.gov/state/analysis.php?sid=FL#:~:text=In%202022%2C%20Florida%20was%20third,of%20Florida's%20total%20net%20generation.&text=About%20four%2Dfifths%20of%20the,1%20megawatt%20or%20larger)%20facilities.

[18] Global Energy Monitor, Global Integrated Power Tracker, April 2025 release.

[19] W. J. Farmer and A. J. Rix, "Evaluating power system network inertia using spectral clustering to define local area stability," *International Journal of Electrical Power Energy Systems*, vol. 134, p. 107404, 2022. [Online]. Available: https://www.sciencedirect.com/science/article/pii/S0142061521006438